Steady-state analysis including parasitic components and switching losses of buck and boost DC-DC PWM converters under any operating

INT. J. ELECTRONICS, 1994, VOL. 77, NO. 5, 679–701

Steady-state analysis including parasitic components and switching losses of buck and boost DC–DC PWM converters under any operating condition

ALBERTO REATTI†

A detailed analysis of DC–DC buck and boost converters operated both in continuous and discontinuous current modes is reported. Expressions for the voltage transfer functions and efficiencies of these two basic topologies have been derived in a closed form. These equations describe the converter behaviour for both constant output voltage and constant input voltage operation. Voltage transfer functions are derived so that the load regulation characteristics of the converters are closely described, including those for continuous current mode operation. Because of this, they can be effectively used to design a converter circuit responding to any given design specification. Both the equations for the efficiencies and voltage transfer functions are general and the values of the parasitic parameters to be introduced can be found on the component data sheets or derived from simple measurements. Because of this, results of the analysis presented can be effectively used in the optimization of the converter circuit performances. The general approach to the analysis of power converters including parasitic components given in the paper can be applied to any power converter circuit. Theoretical derivations are in good agreement with the results of computer simulations performed by using the PSpice program.

1. Introduction

Engineers in the field of power conversion are working to reduce the volume and weight of power converters. In recent years, many resonant DC–DC converter circuits have been presented (see for example Kazimierczuk *et al.* 1992 and 1993, Kazimierczuk and Wang 1992). The main advantage of these circuits is that switching losses are drastically reduced so their operating frequency can be raised above some hundreds of kilohertz. Unfortunately, these circuits have higher conduction losses than conventional pulsewidth-modulation (PWM) DC–DC circuits, cannot be operated at a constant frequency, and require a high quality-factor inductor to be used. Moreover, new integrated control circuits and power components are mostly developed to be used in PWM converters. For this reason, PWM topologies are still those most commonly produced and industry engineers are developing high power-density circuits derived from the two basic buck and boost topologies, operated at increasing switching frequencies. Since high power-density converters can be achieved only if their efficiencies remain high over the entire load range, it is of primary importance to understand how to control the losses in the converter circuit components. Moreover, a good design can be carried out only if all the parameters affecting the converter transfer function are considered (Liberatore and Reatti 1993). In spite of this, the many books and papers written on switch-mode power supplies do not give any general equation for converter efficiencies (see

Received 30 November 1993; accepted 3 February 1994.

†Department of Electronic Engineering, University of Florence, Via di S. Marta, 3, 50139 Florence, Italy.

0020–7217/94 $10.00

Billings 1989, Bracke and Geerling 1986, Fisher 1991, Kassakian *et al.* 1991, Mohan *et al.* 1989), and some of them (Kilgenstein 1989, Pressmann 1991) evaluate the losses in the circuits, their efficiencies and voltage transfer functions under specific conditions, e.g. at the full load operation, and/or by using coarse approximations. Even if this is done according to what is often required by customer design specifications, it does not give a good understanding of the converter behaviour under different operating conditions. Moreover, the voltage transfer function of buck and boost PWM converters operated in continuous current mode (CCM) is generally assumed to be load independent. Due to the parasitics of the converter circuit components, this is not true and variations of voltage transfer functions with load cannot be neglected in those converters supplying a high output current I_O at a low output voltage V_O, e.g. I_O greater than 1 A and $V_O = 3{\cdot}3$ V, 5 V or 12 V. An exact evaluation of efficiency and voltage transfer function cannot be derived by using state-space averaging techniques (see Middlebrook and Ćuk 1981, Mitchell 1988, Lee 1985, Amran *et al.* 1991) because the inductor current ripple is neglected and, as a consequence, power losses in the filter capacitor are not considered. Moreover, the models derived for a frequency domain analysis do not include switching losses, which cannot be neglected when the switching frequency is increased above about 100 kHz. More detailed expressions of PWM converter efficiencies and voltage transfer functions can be found in Czarkowski and Kazimierczuk (1992a–f and 1993), but they only refer to the CCM operation of the PWM converters.

This work presents a systematic method for considering all the major parasitic effects in the evaluation of the efficiency and voltage transfer functions of buck and boost PWM converters. This method has already been used successfully for other converter circuits (see Reatti and Kazimierczuk 1993a, b). Conduction losses are evaluated taking into account the parasitic parameters of the circuit components. The switching losses in the power MOSFET used as a control switch are also considered. Moreover, the expressions for power losses are derived in such a way that the values of parameters to be introduced can be found from component data sheets and/or determined by simple measurements. Thus, the equations presented in this paper can easily be used in designing the converters and to predict the performance of the actual circuit accurately at a high operating frequency for both continuous and discontinuous current mode operation. The significance of the paper is that the results of the analysis presented can be used as a useful tool in the optimization of power converter design.

2. Evaluation of buck and boost DC–DC converter efficiency

2.1. *Assumptions*

The analysis of buck and boost PWM converters is based on the following assumptions.

(*a*) The power MOSFET used as a controllable switch is modelled as an open circuit when OFF and as a constant resistance R_{DS} when ON.

(*b*) The diode is modelled as an open circuit when in the OFF-state and as a series combination of a battery V_F and a resistance R_F when conducting.

(*c*) Passive components like capacitors and inductors are assumed to be linear and time invariant. Moreover, they are assumed to operate at a switching frequency far below their first resonant frequency. The inductor series

resistance R_L and capacitor equivalent series resistance (ESR) R_C are assumed to be independent of operating temperature.

(*d*) Switching losses in the diode are neglected. The reverse recovery effect of fast and ultra-fast diodes is not considered, nor are parasitic capacitances of Schottky diodes.

(*e*) Power consumption of the IC control circuit driving the power MOSFET is not considered.

(*f*) Since the effect of MOSFET parasitic capacitances cannot be neglected, the switching losses have been taken into account.

Figure 1(a) shows the current and voltage waveforms from a PSpice computer simulation of the turn-on of an IRF150 power MOSFET. The switch turn-on can be divided into three time intervals:

(i) during the time interval t_1 the MOSFET drain current i_D increases linearly from zero while the drain-to-source voltage v_{DS} remains constant and is equal to its maximum value V_M;

(ii) during the second time interval t_2 the voltage across the drain and source terminals v_{DS} decreases linearly from V_M; i_D remains constant (the current overshoot is neglected);

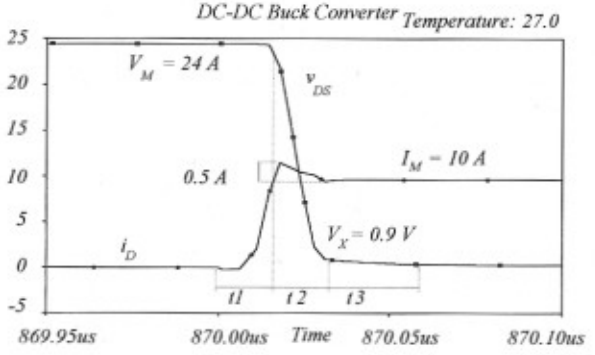

(*a*)

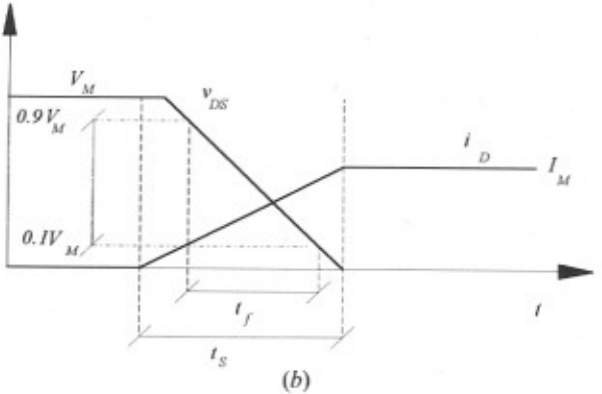

(*b*)

Figure 1. Waveforms of the drain-to-source voltage v_{DS} and drain current during the turn-on of a power MOSFET: (*a*) simulated waveforms; (*b*) approximated waveforms

(iii) time interval t_3 corresponds to the time the voltage v_{DS} takes to decrease from V_X to zero, i_D remaining constant during t_3.

The slope of the waveform of v_{DS} is larger during t_1 than during t_2, because the output parasitic capacitance C_{OSS} increases as v_{DS} decreases. From Fig. 1(*a*) we have $t_1 = 18$ ns, $t_2 = 18$ ns, $t_3 = 72$ ns and $V_X = 0{\cdot}9$ V. The power loss during the MOSFET turn-on process is

$$P_{tON} = P_{t_1} + P_{t_2} + P_{t_3} = \frac{1}{2}(t_1 + t_2) V_M I_M f + \frac{1}{2} t_3 V_X I_M f \tag{1}$$

where f is the MOSFET switching frequency. Since $V_M = 24$ V and $I_M = 10$ A, for a switching frequency $f = 100$ kHz the turn-on power loss is $P_{tON} = 0{\cdot}216 + 0{\cdot}216 + 0{\cdot}032 = 0{\cdot}464$ W.

Turn-on losses can also be evaluated by using the plots in the MOSFET data sheets as follows. From the linearized MOSFET transfer characteristic, which gives the drain current i_D against the gate-to-source voltage v_{GS}, it can be seen that the drain current reaches the value I_M for a certain value of the gate-to-source voltage $v_{GS} = V_{GS}$. Once V_{GS} is known, the plots of v_{GS} against Q_g allow the charge that is to be injected in the gate terminal Q_{glM} to be determined. Time t_1 is expressed as

$$t_1 = \frac{Q_{glM}}{I_G} \tag{2}$$

where I_G is the average current supplied by the driving circuit during the turn-on. Assuming that $V_x = 0$, t_2 is given by

$$t_2 = \frac{V_M C_{GDmin}}{I_G} \tag{3}$$

where $C_{GDmin} = C_{RSSmin}$ is the gate-to-drain parasitic capacitance evaluated at $V_{DS} = V_M$. The turn-on power loss is evaluated by substituting (2) and (3) in

$$P_{tON} = \frac{1}{2} V_M I_M f (t_1 + t_2) \tag{4}$$

For the IRF150 power MOSFET considered in the example, the drain current $I_M = 10$ A when $V_{GS} = 6$ V, that is, when $Q_{glM} = 12$ nC. Since the average gate current during this time interval is $I_G = 0{\cdot}5$ A, we have $t_1 = 24$ ns. With $C_{GDmin} = 280$ pF, the second time interval $t_2 = 13{\cdot}44$ ns. The resulting turn-on power loss in the MOSFET is $P_{tON} = 0{\cdot}449$ W. Since this result differs only slightly from those given by (1), the approximated expression (4) can be considered suitable for evaluating the MOSFET switching losses. Unfortunately, this requires the power MOSFET driving circuit to be known. For practical purposes one can refer to the approximated voltage and current waveforms shown in Fig. 1(*b*). The turn-on power loss is given by

$$P_{tON} = \frac{1}{6} I_M V_M t_S f = \frac{5}{24} I_M V_M t_f f \tag{5}$$

where t_S is the turn-on time and t_f is the time the drain-to-source voltage takes to decrease from 90% to 10% of the maximum value V_M. Since t_f is given in the

MOSFET data sheets, turn-on power loss can be easily evaluated using (5). From the IRF150 data sheet we have $t_f = 100$ ns for $V_M = 24$ V and $I_M = 20$ A. Using (6) and $I_M = 10$ A and $V_M = 24$ V, the turn-on power loss is evaluated as $P_{tON} = 0{\cdot}5$ W. Note that this value of P_{tON} is only 0·034 W larger than that obtained using (1). Also, turn-off losses can be taken into account by using the value of the rise time t_f of v_{DS} given in the power MOSFET data sheets. As a result, the total switching losses in the MOSFET are

$$P_{SW} = P_{tON} + P_{tOFF} = \frac{5}{24} I_M V_M (t_f + t_r) f \tag{6}$$

Actually, snubber circuits and parasitic components modify the switching voltage and current waveforms of the MOSFET. However, when proper operation of the converter is achieved the current and voltage overshoots are relatively small. Moreover, by using snubber circuits, switching losses are transferred from the power switch to the snubber components. Therefore, (6) gives the overall switching losses to a good approximation. The main advantage of using (6) is that the values of t_f and t_r can be read directly from the MOSFET data sheets and the switching power losses evaluated regardless of the driving circuit.

2.2. *Buck converter operated in the continuous current mode*

A schematic of a DC–DC circuit buck converter circuit and its equivalent circuit are shown in Fig. 2(*a*) and (*b*), respectively. The voltage and current waveforms over

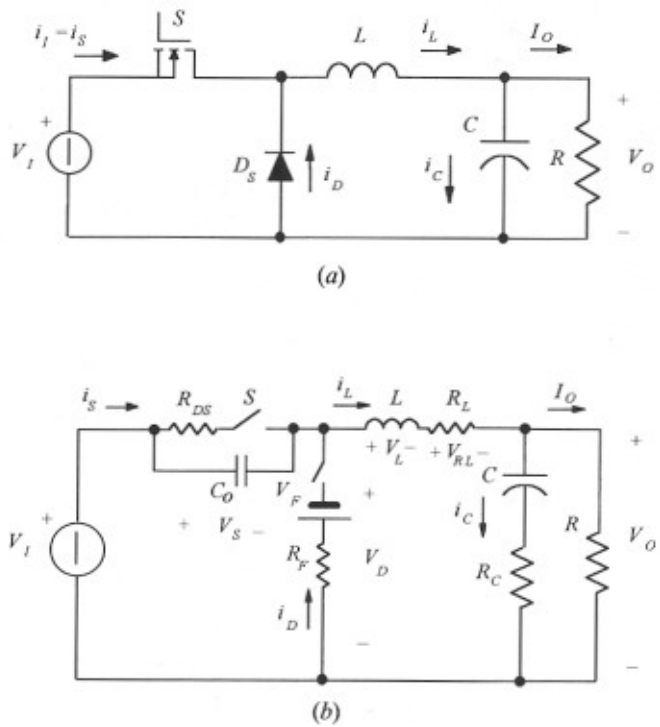

Figure 2. PWM DC–DC buck converter: (*a*) ideal circuit; (*b*) equivalent circuit including the parasitic components.

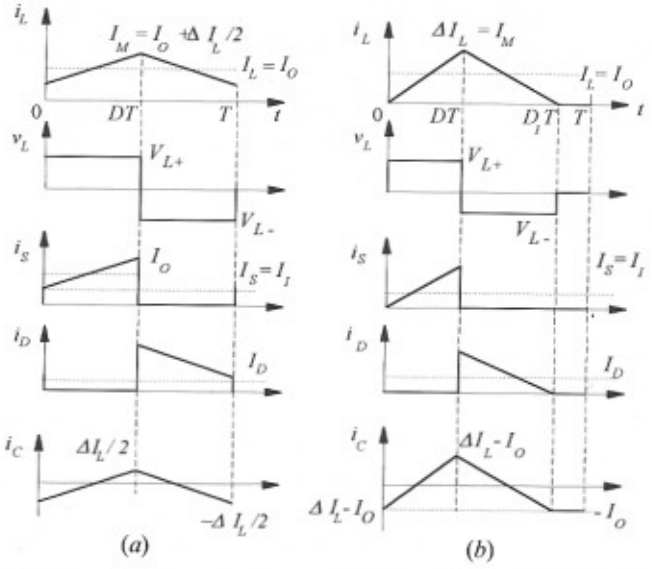

Figure 3. Steady-state current and voltage waveforms in a PWM buck converter. (*a*) continuous current mode; (*b*) discontinuous current mode.

one switching period of a buck converter operated in the CCM are shown in Fig. 3(*a*). The current through the inductor L in the circuit of Fig. 2(*a*) is given by

$$i_L(t) = \begin{cases} \dfrac{V_O(1-D)}{LD}t + \left[I_O - \dfrac{1}{2}\dfrac{V_O(1-D)}{Lf}\right] & \text{for} \quad 0 < t \le DT \\ -\dfrac{V_O}{L}(t-DT) + \left[I_O + \dfrac{1}{2}\dfrac{V_O(1-D)}{Lf}\right] & \text{for} \quad DT < t \le T \end{cases} \tag{7}$$

where I_O is the DC output current, $D = t_{on}/T$ is the MOSFET ON duty cycle, and T and f are the converter switching period and frequency, respectively. The RMS value of the current through L is

$$I_{L,RMS} = \left[I_O^2 + \frac{V_O^2(1-D)^2}{12L^2f^2}\right]^{1/2} \tag{8}$$

Therefore, the power loss in the inductor equivalent resistance is

$$P_{RL} = R_L I_{L,RMS}^2 = R_L\left[I_O^2 + \frac{V_O^2(1-D)^2}{12L^2f^2}\right] \tag{9}$$

As shown in Fig. 3(*a*), the current through the power MOSFET is that through the inductor when $0 < t \le DT$. Therefore, the RMS value of the switch current is $I_{S,RMS} = I_{L,RMS}D^{1/2}$. Moreover, the peak current is $I_M = I_O + V_O(1-D)/2Lf$ and the power losses in the MOSFET are

$$P_M = P_{RDS} + P_{SW} = R_{DS} I_{S,RMS}^2 + \frac{5}{24} V_M I_M (t_f + t_r) f$$

$$= R_{DS} D \left[I_O^2 + \frac{V_O^2 (1-D)^2}{12 L^2 f^2} \right] + \frac{5}{24} V_I \left(I_O + \frac{V_O (1-D)}{2Lf} \right) (t_f + t_r) f \tag{10}$$

Since the inductor current flows through the diode when $DT < t \leq T$, the average and the RMS values of the current through the diode are $I_{D,AVG} = (1-D) I_O$ and $I_{D,RMS} = (I-D)^{1/2} I_{L,RMS}$, respectively. As a result, conduction losses in the diode are expressed as

$$P_D = V_F I_{D,AVG} + R_F I_{D,RMS}^2 = V_F (1-D) I_O + R_F (1-D) \left[I_O^2 + \frac{V_O^2 (1-D)^2}{12 L^2 f^2} \right] \tag{11}$$

Only the AC component of the diode current flows through filter capacitor C, resulting in a power loss in the capacitor ESR given by

$$P_{RC} = R_C I_{C,RMS}^2 = R_C \left[\frac{V_O^2 (1-D)^2}{12 L^2 f^2} \right] \tag{12}$$

From Fig. 2(*b*) we have

$$\left.\begin{aligned} V_I - V_S - V_{RL} - V_{L+} - V_O = 0 \quad \text{for} \quad 0 < t \leq DT \\ V_D + V_{RL} + V_L + V_O = 0 \quad \text{for} \quad D < t \leq T \end{aligned}\right\} \tag{13}$$

where V_{L+} and V_{L-} are the equivalent voltages across L during the switch ON and OFF times, respectively. Voltages V_S, V_{RL}, V_D are the RMS values of the voltage drops across the power MOSFET, the inductor series resistance and the diode, respectively. The voltage drop across the filter capacitor ESR has been neglected because DC–DC converter design specifications require that the maximum AC ripple of the DC output voltage is very small, e.g. less than 1% of the nominal DC output voltage. Using (8) and (9), the RMS equivalent voltage drop across the inductor resistance is

$$V_{RL} = \frac{P_{RL}}{I_{L,RMS}} = R_L \left[I_O^2 + \frac{V_O^2 (1-D)^2}{12 L^2 f^2} \right]^{1/2} \tag{14}$$

The voltage drops across the power MOSFET and diode are given by

$$V_S = \frac{P_{RDS}}{I_{S,RMS}} = R_{DS} \left\{ D \left[I_O^2 + \frac{V_O^2 (1-D)^2}{12 L^2 f^2} \right] \right\}^{1/2} \tag{15}$$

and

$$V_D = \frac{P_D}{I_{D,RMS}} = R_F \left\{ (1-D) \left[I_O^2 + \frac{V_O^2 (1-D)^2}{12 L^2 f^2} \right] \right\}^{1/2} + \frac{V_F (1-D)^{1/2}}{\left(1 + \dfrac{V_O^2 (1-D)^2}{12 L^2 f^2 I_O^2} \right)^{1/2}} \tag{16}$$

respectively. Moreover, in the steady-state operation we have

$$V_{L+} D = |V_{L-}| (1-D) \tag{17}$$

and, therefore, the input voltage is expressed as

$$V_I=\frac{1}{D}[V_O+V_S D+V_{RL}+V_D(1-D)]=\frac{V_O}{D}+\frac{1}{D}[DR_{DS}D^{1/2}+R_L+R_F(1-D)(1-D)^{1/2}$$
$$\times\left(I_O^2+\frac{V_O^2(1-D)^2}{12L^2f^2}\right)^{1/2}+\frac{V_F(1-D)(1-D)^{1/2}}{D\left(\frac{1+V_O^2(1-D)^2}{12L^2f^2I_O^2}\right)^{1/2}} \tag{18}$$

The efficiency of a DC–DC converter is

$$\eta\equiv\frac{P_O}{P_I}=\frac{P_O}{P_O+P_{RL}+P_M+P_D+P_{RC}} \tag{19}$$

Substitution of (9)–(12) in (19) gives the efficiency of a DC–DC buck converter operated in the CCM

$$\eta_{BUCCM}=\left\{1+\frac{V_F}{V_O}(1-D)+[R_L+R_{DS}D+R_F(1-D)]\frac{I_O}{V_O}+[R_L+R_{DS}D+R_F(1-D)+R_C]\right.$$
$$\left.\times\frac{(1-D)^2}{12L^2f^2}\frac{V_O}{I_O}+\frac{5}{24}V_I\left[\frac{1}{V_O}+\frac{(1-D)}{2Lf\,I_O}\right](t_r+t_f)f\right\}^{-1} \tag{20}$$

Assuming a load resistance $R=V_O/I_O$ and neglecting the switching losses and the current ripple, (20) simplifies as

$$\eta'_{BUCCM}=\left[1+\frac{V_F(1-D)}{V_O}+\frac{R_L+R_{DS}D+R_F(1-D)}{R}\right]^{-1} \tag{21}$$

This simplified expression can be used effectively when L is large and the switching frequency low.

The voltage transfer function of the buck converter $M_{VBUCCM}=V_O/V_I$ could be evaluated by using (18). However, the resulting expression would be largely approximated at high operating frequencies because switching losses are not considered. The voltage transfer function of a DC–DC converter can be evaluated more precisely by using the following definition of the efficiency:

$$\eta\equiv\frac{P_O}{P_I}=\frac{I_O V_O}{I_I V_I}=M_V M_I \tag{22}$$

where M_V and M_I are the voltage and current transfer functions, respectively.

Since the current transfer function of a buck converter operated in the CCM is $M_{IBUCCM}\equiv I_O/I_I=I_L/I_S=1/D$, using (20) and (22) the steady-state voltage transfer function of a non-ideal buck converter operated in the CCM is

$$M_{\text{VBUCCM}}=\frac{\eta_{\text{BUCCM}}}{M_{\text{IBUCCM}}}=\eta_{\text{BUCCM}}D$$

$$=D\left\{1+\frac{V_F}{V_O}(1-D)+[R_L+R_{DS}D+R_F(1-D)]\frac{I_O}{V_O}+[R_L+R_{DS}D+R_F(1-D)+R_C]\right.$$

$$\left.\times\frac{(1-D)^2}{12L^2f^2}\frac{V_O}{I_O}+\frac{5}{24}V_I\left[\frac{1}{V_O}+\frac{(1-D)}{2Lf\,I_O}\right](t_r+t_f)f\right\}^{-1} \tag{23}$$

This expression is simplified if the switching losses and the current ripple are negligible (that is, for a low frequency operation with large values of L)

$$M'_{\text{VBUCCM}}=D\left[1+\frac{V_F(1-D)}{V_O}+\frac{R_L+R_{DS}D+R_F(1-D)}{R}\right]^{-1} \tag{24}$$

By using (18) the efficiency and the voltage transfer function of the buck converter are expressed in a closed form for both constant input voltage and constant output voltage operation.

As an example, a buck converter operated in the CCM at a switching frequency $f=100\,\text{kHz}$, an input voltage $V_I=28\,\text{V}$ and a constant nominal output voltage $V_O=10\,\text{V}$ ($D\cong 0{\cdot}36$), supplying a maximum output current $I_O=12\,\text{A}$, was considered. It was assumed that the MOSFET drain-to-source resistance was $R_{DS}=55\,\text{m}\Omega$, the voltage of the battery and resistance used in the diode equivalent circuit were $V_F=0{\cdot}57\,\text{V}$ and $R_F=20\,\text{m}\Omega$, respectively. The choke inductor had an inductance $L=50\,\mu\text{H}$ and a parasitic resistance $R_L=50\,\text{m}\Omega$. The capacitor ESR was $R_C=50\,\text{m}\Omega$. Figure 4 compares the efficiencies of the converter evaluated according to (20) and (21). Since the switching losses and the contribution of the current ripple to the current RMS value are neglected in (21), η'_{BUCCM} is higher than η_{BUCCM} over the

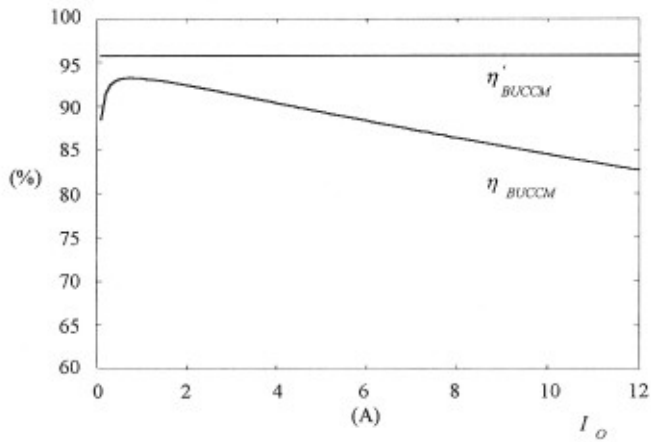

Figure 4. Efficiencies η'_{BUCCM} and η_{BUCCM} of a buck converter operated in the CCM, a constant output voltage $V_O=10\,\text{V}$ as a function of the DC output current I_O at $f=200\,\text{kHz}$, $R_{DS}=55\,\text{m}\Omega$, $t_r=t_f=80\,\text{ns}$, $V_F=0{\cdot}57\,\text{V}$, $R_F=20\,\text{m}\Omega$, $L=50\,\mu\text{H}$, $R_L=50\,\text{m}\Omega$ and $R_C=50\,\text{m}\Omega$.

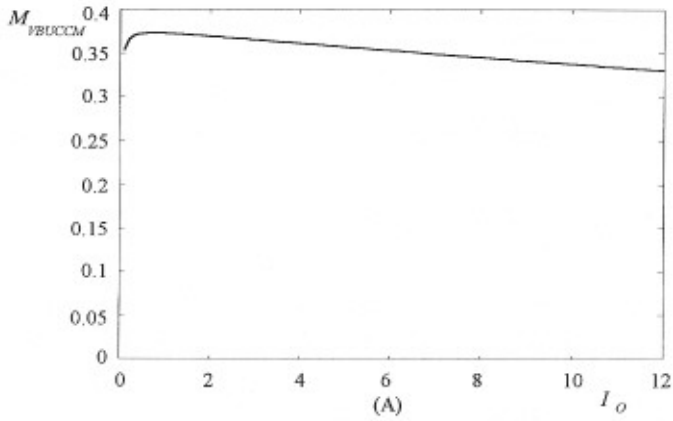

Figure 5. Voltage transfer function M_{VBUCCM} of a buck converter operated in the CCM, a constant output voltage $V_O = 10\,V$ as a function of the DC output current I_O at $f = 200\,kHz$, $R_{DS} = 55\,m\Omega$, $t_r = t_f = 80\,ns$, $V_F = 0{\cdot}57\,V$, $R_F = 20\,m\Omega$, $L = 50\,\mu H$, $R_L = 50\,m\Omega$ and $R_C = 50\,m\Omega$.

entire load range. Moreover, the latter decreases when the output current increases, while the former is almost constant over the entire load range. Figure 5 shows that voltage transfer function M_{VBUCCM} shown for a constant output voltage ($V_O = 10\,V$), depends on the output power. Actually, the voltage drops in the parasitic components increase as the output current rises from zero to its maximum value. Figure 6 shows the voltage transfer function against the output current I_O with the duty cycle D used as a parameter for a buck converter circuit operated at a constant input voltage. It is shown that the voltage transfer function is zero if the duty cycle is as low as 0·1 and the output current higher than 5 A. This is because a high current in the parasitic components produces an overall voltage drop which is higher than the

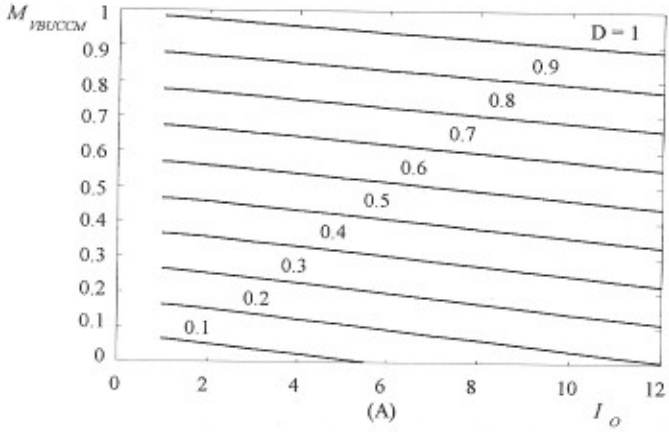

Figure 6. Voltage transfer function M_{VBUCCM} of a buck converter operated in the CCM, a constant input voltage $V_I = 28\,V$ as a function of the DC output current I_O with the duty cycle D used as a parameter at $f = 200\,kHz$, $R_{DS} = 55\,m\Omega$, $t_r = t_f = 80\,ns$, $V_F = 0{\cdot}57\,V$, $R_F = 20\,m\Omega$, $L = 50\,\mu H$, $R_L = 50\,m\Omega$ and $R_C = 50\,m\Omega$.

achievable DC output voltage at $D=0{\cdot}1$. In Fig. 7 the efficiency of a buck converter is plotted as a function of the output current using the duty cycle D as parameter. The efficiency decreases to zero when the overall converter voltage drop is equal to the DC output voltage.

2.3. *Buck converter operated in the discontinuous current mode*

The current and voltage waveforms for a buck converter operated in discontinuous current mode (DCM) are shown in Fig. 3(*b*). The current through the inductor L has a triangular waveform with a maximum value

$$I_M=\frac{V_O(D_1-D)}{Lf} \tag{25}$$

where D_1 is expressed as (Fisher 1991)

$$D_1=\frac{D}{2}\left[1+\left(1+\frac{8I_OLf}{V_OD^2}\right)\right]^{1/2} \tag{26}$$

Since the RMS value of the inductor current is $I_{L,RMS}=I_M(D_1/3)^{1/2}$, the power loss in the inductor ESR is

$$P_{RL}=R_LI_{L,RMS}^2=R_L\frac{D_1}{3}\left[\frac{V_O(D_1-D)}{Lf}\right]^2 \tag{27}$$

The MOSFET is ON when $0<t\le DT$. Therefore, the RMS value of the current through the power MOSFET is $I_{S,RMS}=I_{L,RMS}(D/D_1)^{1/2}$, and the total power loss in the power MOSFET is given by

$$P_M=R_{DS}I_{S,RMS}^2+\frac{5}{24}V_MI_M(t_f+t_r)f=R_{DS}\frac{D}{3}\left[\frac{V_O(D_1-D)}{Lf}\right]^2+\frac{5}{24}V_1\frac{V_O(D_1-D)}{Lf}(t_f+t_r)f \tag{28}$$

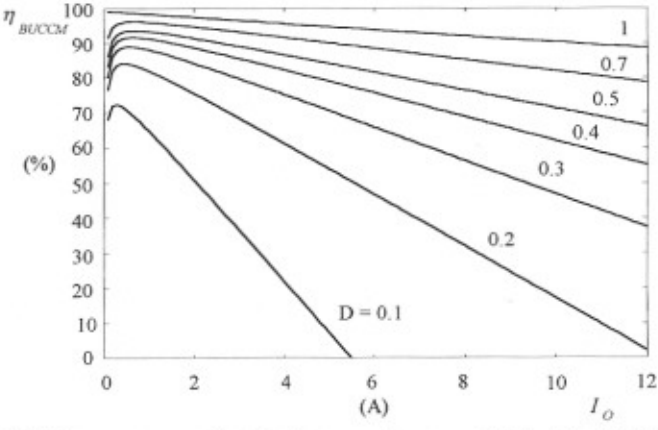

Figure 7. Efficiency η_{BUCCM} of a buck converter operated in the CCM, a constant input voltage $V_I=28$ V as a function of the DC output current I_O with the duty cycle D used as a parameter at $f=200$ kHz, $R_{DS}=55$ mΩ, $t_r=t_f=80$ ns, $V_F=0{\cdot}57$ V, $R_F=20$ mΩ, $L=50$ μH, $R_L=50$ mΩ and $R_C=50$ mΩ.

Similarly, the conduction power loss in the diode is expressed as

$$P_D = V_F I_{D,AVG} + R_F I_{D,AVG}^2 = V_F \frac{V_O(D_1 - D)^2}{2Lf} + R_F \frac{V_O^2(D_1 - D)^3}{3L^2 f^2} \tag{29}$$

because D_S is ON when $DT < t \leq D_1 T$. Since capacitor C conducts the AC component of the current through the diode, the power loss in the capacitor ESR is

$$P_{RC} = R_C I_{C,RMS}^2 = R_C \frac{V_O^2(D_1 - D)^2(4D_1 - 3D_1^2)}{12L^2 f^2} \tag{30}$$

Combining (13) (where the second equation is now true for $DT < t \leq D_1 T$) with $V_{L+} D = |V_{L-}|(D_1 - D)$ and evaluating the equivalent voltage drops across the parasitic components yields the expression for the input voltage

$$V_I = V_O \frac{D_1}{D} + \left[R_{DS} D^{1/2} + R_L \frac{D_1}{D} D_1^{1/2} + R_F \frac{(D_1 - D)}{D} (D_1 - D)^{1/2} \right] \times \frac{V_O(D_1 - D)}{\sqrt{3}Lf} + \frac{V_F \sqrt{3}(D_1 - D)^{3/2}}{2D} \tag{31}$$

Substitution of (27)–(30) in (19) yields the efficiency of the buck converter operated in the DCM

$$\eta_{BUDCM} = \left\{ 1 + V_F \frac{(D_1 + D)^2}{2I_O Lf} + \left[R_L D_1 + R_F(D_1 - D) + R_{DS} D + R_C D_1 \left(1 - \frac{3D_1}{4} \right) \right] \times \frac{V_O(D_1 - D)^2}{3I_O L^2 f^2} + \frac{5}{24} V_I \frac{(D_1 - D)}{I_O Lf} (t_r + t_f) f \right\}^{-1} \tag{32}$$

Since the current transfer function of a boost converter operated in the DCM is $M_{IBUCCM} = I_O / I_I = D_1 / D$, the voltage transfer function is given as

$$M_{VBUDCM} = \frac{\eta_{BUDCM}}{M_{IBUDCM}} = \frac{D_1}{D} \left\{ 1 + \frac{V_F(D_1 - D)^2}{2I_O Lf} + \left[R_L D_1 + R_F(D_1 - D) + R_{DS} D + R_C D_1 \left(1 - \frac{3D_1}{4} \right) \right] \times \frac{V_O(D_1 - D)^2}{3I_O L^2 f^2} + \frac{5}{24} V_I \frac{(D_1 - D)}{I_O Lf} (t_r + t_f) f \right\}^{-1} \tag{33}$$

Figures 8 and 9 show the efficiency and the voltage transfer function of a DC–DC buck converter operated in DCM at an input voltage $V_I = 28\,\text{V}$, a nominal output voltage and current $V_O = 10\,\text{V}$ and $I_O = 3\,\text{A}$, respectively. The switching frequency was $f = 50\,\text{kHz}$, the rise and fall times were $t_r = t_f = 80\,\text{ns}$, the inductor had an inductance $L = 10\,\mu\text{H}$ and an equivalent series resistance $R_L = 50\,\text{m}\Omega$, the MOSFET drain-to-source resistance was $R_{DS} = 55\,\text{m}\Omega$, the capacitor ESR was $R_C = 50\,\text{m}\Omega$, the battery of the diode model had $V_F = 0{\cdot}57$ and the resistance $R_F = 20\,\text{m}\Omega$.

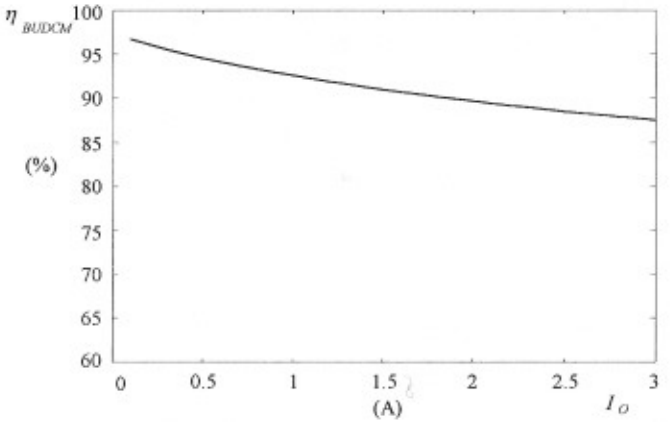

Figure 8. Efficiency η_{BUDCM} of a buck converter operated in the DCM, a constant input voltage $V_I = 28$ V as a function of the DC output current I_O, at $f = 50$ kHz, $R_{DS} = 55$ mΩ, $t_r = t_f = 80$ ns, $V_F = 0{\cdot}57$ V, $R_F = 20$ mΩ, $L = 10$ μH, $R_L = 50$ mΩ and $R_C = 50$ mΩ.

2.4. *Boost converter operated in the continuous current mode*

A schematic of a PWM DC–DC boost converter circuit is shown in Fig. 10(*a*). The current and voltage waveforms of the converter operated in the CCM are depicted in Fig. 11(*a*). The equivalent circuit of the boost converter including the parasitic components is shown in Fig. 10(*b*).

The power losses in the series resistance of inductor L are

$$P_{RL} = R_L I_{L,RMS}^2 = R_L \left[\frac{I_O^2}{(1-D)^2} + \frac{V_I^2 D^2}{12 L^2 f^2} \right] \tag{34}$$

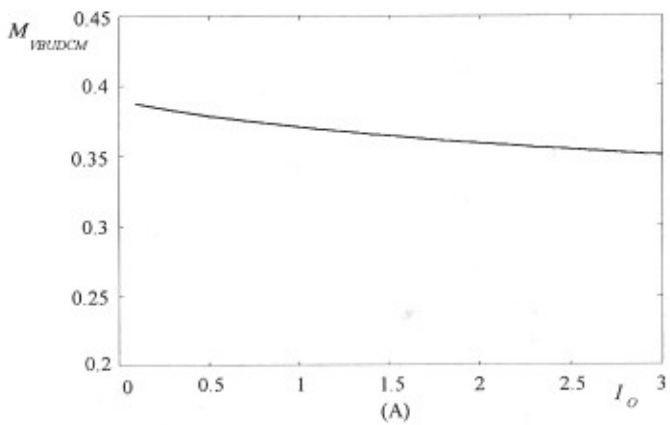

Figure 9. Voltage transfer function M_{VBUDCM} of a buck converter operated in the DCM, a constant input voltage $V_I = 28$ V as a function of the DC output current I_O, $f = 50$ kHz, $R_{DS} = 55$ mΩ, $t_r = t_f = 80$ ns, $V_F = 0{\cdot}57$ V, $R_F = 20$ mΩ, $L = 10$ μH, $R_L = 50$ mΩ and $R_C = 50$ mΩ.

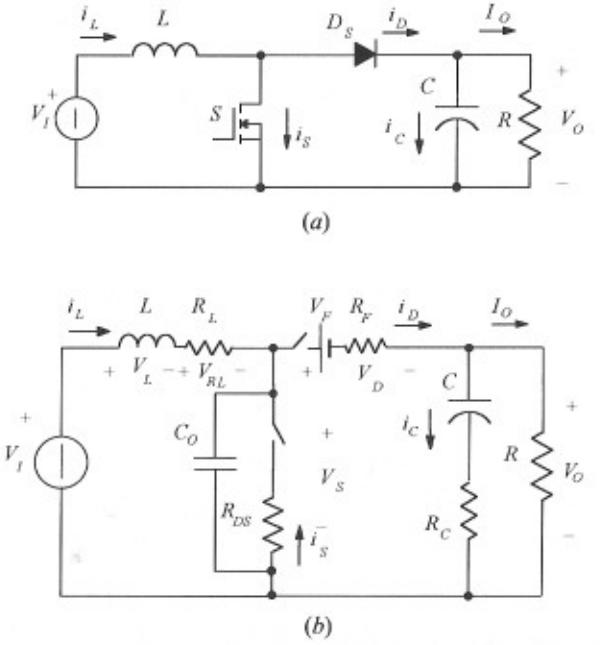

Figure 10. PWM DC–DC boost converter: (*a*) ideal circuit; (*b*) equivalent circuit including the parasitic components.

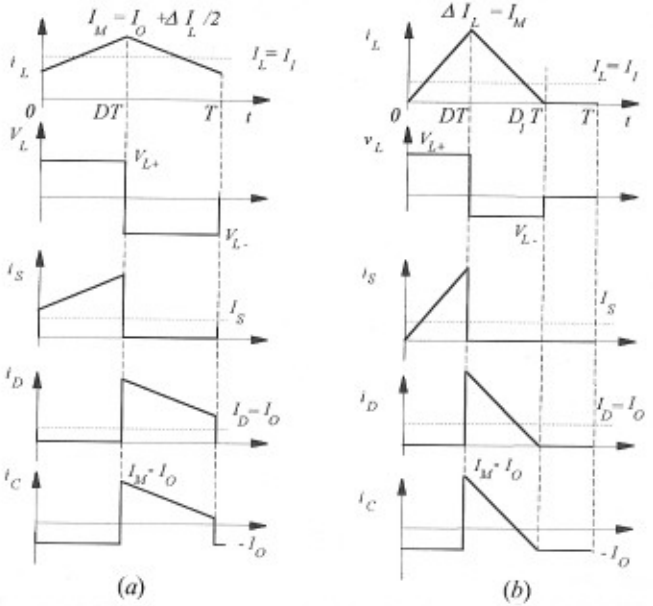

Figure 11. Steady-state current and voltage waveforms in a PWM boost converter: (*a*) continuous current mode; (*b*) discontinuous current mode.

The current i_S through the power MOSFET is equal to i_L during the time interval $0 < t \le DT$ and then is zero. Therefore, the RMS value of i_S is $I_{S,RMS} = I_{L,RMS} D^{1/2}$, the maximum voltage across the switch is $V_M = V_O$, and the power loss in the MOSFET is given by

$$P_M = R_{DS} I_{S,RMS}^2 + \frac{5}{24} V_M I_M (t_r + t_f) f$$

$$= R_{DS} D \left[\frac{I_O^2}{(1-D)^2} + \frac{V_I^2 D^2}{12 L^2 f^2} \right] + \frac{5}{24} V_O \left[\frac{I_O}{(1-D)} + \frac{V_I D}{2Lf} \right] (t_r + t_f) f \tag{35}$$

Since the inductor current flows through D_S when $DT < t \le T$, the average and RMS values of the diode current are $I_{D,AVG} = I_O$ and $I_{D,RMS} = I_{L,RMS}(1-D)^{\frac{1}{2}}$, respectively. Therefore, power loss in D_S is

$$P_D = V_F I_{D,AVG} + R_F I_{D,RMS}^2 = R_F (1-D) \left[\frac{I_O^2}{(1-D)^2} + \frac{V_I^2 D^2}{12 L^2 f^2} \right] + V_F I_O \tag{36}$$

The power loss in the filter capacitor ESR is expressed as

$$P_{RC} = R_C I_{C,RMS}^2 = R_C D (1-D) \left[\frac{I_O^2}{(1-D)^2} + \frac{V_I^2 D}{12 L^2 f^2} \right] \tag{37}$$

By using (17), evaluating the equivalent voltage drops across the converter parasitic elements, and neglecting the inductor current ripple, the input voltage is

$$V_I = V_O (1-D) + [R_{DS} D (D)^{1/2} + R_L + R_F (1-D)^{1/2}] \frac{I_O}{1-D} + V_F (1-D)^{3/2} \tag{38}$$

Combining (34)–(37) and (19) gives the efficiency of the boost converter operated in the CCM

$$\eta_{BOCCM} = \left\{ 1 + \frac{V_F}{V_O} + [R_L + R_{DS} D + R_F (1-D) + R_C D (1-D)] \frac{I_O}{V_O} \frac{1}{(1-D)^2} \right.$$

$$+ [R_L + R_{DS} D + R_F (1-D) + R_C D (1-D)] \frac{(1-D)^2}{12 L^2 f^2} \frac{V_I}{I_O} + \frac{5}{24}$$

$$\left. \times \left[\frac{1}{(1-D)} + \frac{V_I}{2Lf I_O} \right] (t_r + t_f) f \right\}^{-1} \tag{39}$$

Substitution of $M_{IBOCCM} = (1-D)$ and (39) in (22) yields the converter voltage transfer function

$$M_{VBOCCM} = \frac{1}{1-D} \left\{ 1 + \frac{V_F}{V_O} + [R_L + R_{DS} D + R_F (1-D) + R_C D (1-D)] \frac{I_O}{V_O} \frac{1}{(1-D)^2} \right.$$

$$+ [R_L + R_{DS} D + R_F (1-D) + R_C D (1-D)] \frac{(1-D)^2}{12 L^2 f^2} \frac{V_I}{I_O} + \frac{5}{24}$$

$$\left. \times \left[\frac{1}{(1-D)} + \frac{V_I}{2Lf I_O} \right] (t_r + t_f) f \right\}^{-1} \tag{40}$$

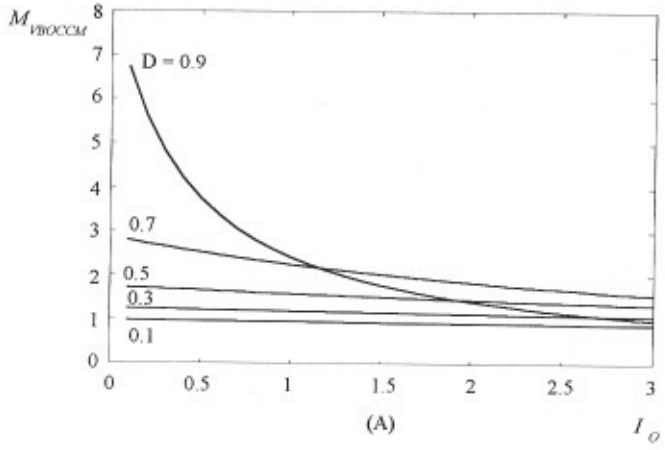

Figure 12. Voltage transfer function M_{VBOCCM} of a boost converter operated in the CCM, a constant output voltage $V_O = 12\,V$ as a function of the DC output current I_O with the duty cycle D used as a parameter at $f = 100\,kHz$, $R_{DS} = 55\,m\Omega$, $t_r = t_f = 100\,ns$, $V_F = 1{\cdot}66\,V$, $R_F = 30\,m\Omega$, $L = 200\,\mu H$, $R_L = 300\,m\Omega$ and $R_C = 20\,m\Omega$.

By using (38), both the efficiency and the voltage transfer function are expressed in a closed form for constant output, and input, voltage operation.

Figure 12 plots the voltage transfer function M_{VBOCCM} of a boost converter operated in the CCM as a function of the DC output current I_O, by using the duty cycle D as a parameter. It was assumed that the converter was operated at a constant output voltage $V_O = 12\,V$, a maximum output current $I_O = 3\,A$ and a switching frequency $f = 100\,kHz$. An inductance $L = 200\,\mu H$ was selected with a parasitic resistance $R_L = 0{\cdot}3\,\Omega$. The MOSFET drain-to-source resistance was $R_{DS} = 55\,m\Omega$ and switching times were $t_r = t_f = 100\,ns$. The diode equivalent circuit had a battery voltage $V_F = 1{\cdot}66\,V$ and a resistance $R_F = 30\,m\Omega$. Filter capacitor ESR was $R_C = 20\,m\Omega$. Figure 12 shows clearly that the voltage transfer function of the DC–DC boost converter was almost load independent only for values of the duty cycle D lower than 0·5, even in the case of a relatively low output current. In Fig. 13 the transfer function obtained from the analysis of the ideal boost converter (see Mohan *et al.* 1989 and Fisher 1991, as examples) is plotted as a function of D and compared to that obtained considering all parasitic components in the converter circuit at different values of output current I_O. Even at a low output current, $I_O = 0{\cdot}1\,A$, the voltage transfer function was not greater than nine and was zero when $D = 1$. Moreover, for the full load operation, the voltage transfer function was not higher than 1·6, that is, the minimum voltage the converter could be operated at was $V_I = 7{\cdot}5\,V$. The converter efficiency is plotted against the output current by using duty cycle D as a parameter in Fig. 14. The boost converter operated in the CCM had a high efficiency over the entire load range if the duty cycle D was lower than $D = 0{\cdot}5$. In Fig. 15 the converter efficiency is plotted as a function of the duty cycle D by using the output current I_O as a parameter. Figures 13–15 show that the converter can be operated with high efficiency for input voltage V_I ranging from 9 V to 12 V.

2.5. *Boost converter operated in the discontinuous current mode*

The RMS values of the current through the converter components are evaluated from the waveforms in Fig. 11(*b*). The power loss in the inductor L is expressed as

$$P_{RL}=R_L I_{L,RMS}^2=R_L I_M^2\frac{D_1}{3}=R_L\frac{V_I^2D^2}{L^2f^2}\frac{D_1}{3} \tag{41}$$

where I_M is the maximum current through the converter components and (from Fisher 1991)

$$D_1=D+\frac{I_OLf}{V_OD}+\left[\left(\frac{I_OLf}{V_OD}\right)^2+2\frac{I_OLf}{V_O}\right]^{1/2} \tag{42}$$

As in a buck converter, the RMS current in the MOSFET is $I_{S,RMS}=I_{L,RMS}D^{1/2}$. Therefore, the power loss in the MOSFET is

$$P_M=R_{DS}\frac{V_I^2D^2}{L^2f^2}\frac{D}{3}+\frac{5}{24}V_O\frac{V_ID}{L}(t_r+t_f) \tag{43}$$

Since the average value of the current through diode D_S is $I_D=I_O$ and the RMS value of the diode current is $I_{D,RMS}=I_{L,RMS}((D_1-D)/D_1)^{1/2}$, the power loss in the diode D_S is

$$P_D=V_FI_O+R_F\frac{V_I^2D^2}{L^2f^2}\frac{D_1-D}{3} \tag{44}$$

The AC component of the current i_D flows through filter capacitor C and the power loss in its ESR is

$$P_{RC}=R_C\left[I_O^2+\frac{V_I^2D^2}{L^2f^2}\frac{D_1-D}{3}-I_O\frac{V_ID}{Lf}(D_1-D)\right] \tag{45}$$

By evaluating the equivalent voltage drops across the parasitic components of the circuit of Fig. 2(*b*), the expression for the input voltage is

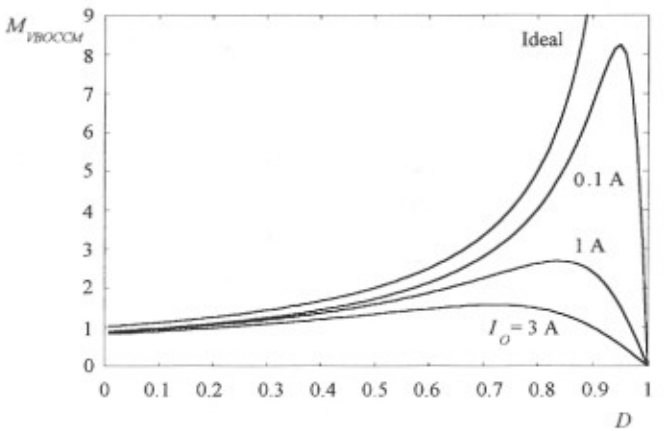

Figure 13. Voltage transfer function M_{VBOCCM} of a boost converter operated in the CCM, a constant output voltage $V_O=12$ V as a function of the duty cycle D with the DC output current I_O used as a parameter at $f=100$ Hz, $R_{DS}=55$ mΩ, $t_r=t_f=100$ ns, $V_F=1{\cdot}66$ V, $R_F=30$ mΩ, $L=200$ μH, $R_L=300$ mΩ and $R_C=20$ mΩ.

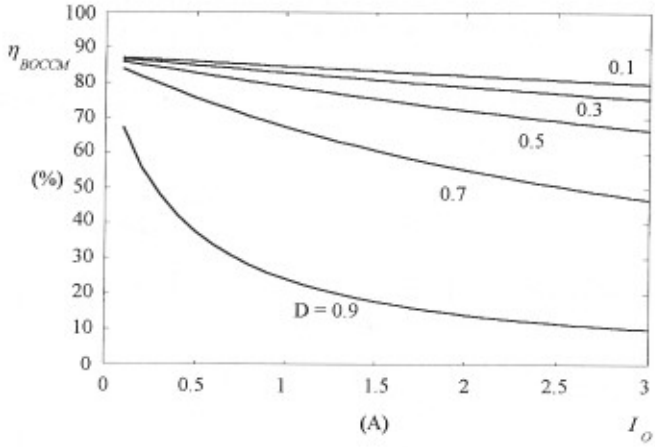

Figure 14. Efficiency η_{BOCCM} of a boost converter operated in the CCM, a constant output voltage $V_O = 12\,V$ as a function of the DC output current I_O with the duty cycle D used as a parameter at $f = 100\,kHz$, $R_{DS} = 55\,m\Omega$, $t_r = t_f = 100\,ns$, $V_F = 1{\cdot}66\,V$, $R_F = 30\,m\Omega$, $L = 200\,\mu H$, $R_L = 300\,m\Omega$ and $R_C = 20\,m\Omega$.

$$V_1 = \frac{D_1 - D}{2D_1K}V_O + \left[\left(\frac{D_1 - D}{2D_1K}V_O\right)^2 + \frac{(D_1 - D)^{1/2}}{\sqrt{3D_1D}}\frac{V_F I_O L f}{K}\right]^{1/2} \tag{46}$$

where

$$K = 1 - \frac{D_1}{D}\frac{1}{\sqrt{3Lf}}[R_L D_1^{3/2} + R_{DS}D^{3/2} + R_F(D_1 - D)^{3/2}] \tag{47}$$

Combining (41), (43)–(45) and (19) gives the efficiency of the converter operated in the DCM

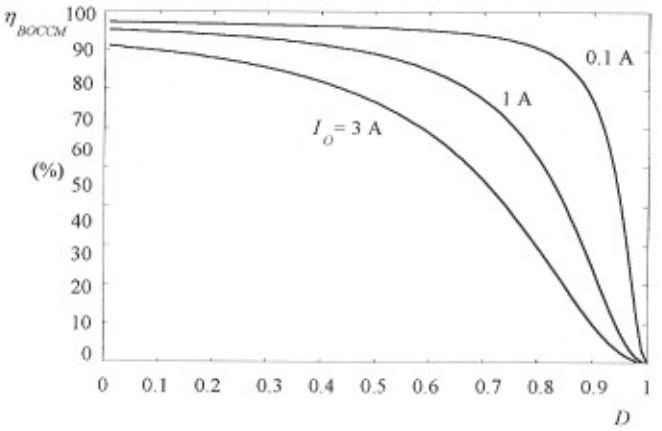

Figure 15. Efficiency η_{BOCCM} of a boost converter operated in the CCM, a constant output voltage $V_O = 12\,V$ as a function of the duty cycle D with the DC output current I_O used as a parameter at $f = 100\,kHz$, $R_{DS} = 55\,m\Omega$, $t_r = t_f = 100\,ns$, $V_F = 1{\cdot}66\,V$, $R_F = 30\,m\Omega$, $L = 200\,\mu H$, $R_L = 300\,m\Omega$ and $R_C = 20\,m\Omega$.

$$\eta_{\mathrm{BODCM}}=\left\{1+\frac{V_{\mathrm{F}}}{V_{\mathrm{O}}}+[R_{\mathrm{L}}D_1+R_{\mathrm{DS}}D+R_{\mathrm{F}}(D_1-D)+R_{\mathrm{C}}(D_1-D)]\right.$$

$$\left.\times\frac{V_{\mathrm{I}}^2}{V_{\mathrm{O}}I_{\mathrm{O}}}\frac{D^2}{3L^2f^2}+R_{\mathrm{C}}\left[\frac{I_{\mathrm{O}}}{V_{\mathrm{O}}}-\frac{V_{\mathrm{I}}D(D_1-D)}{V_{\mathrm{O}}Lf}\right]+\frac{5}{24}\frac{V_{\mathrm{I}}D}{LfI_{\mathrm{O}}}(t_{\mathrm{r}}+t_{\mathrm{f}})f\right\}^{-1} \tag{48}$$

The voltage transfer function of a boost converter operated in the DCM is

$$M_{\mathrm{VBODCM}}=\frac{\eta_{\mathrm{BODCM}}}{M_{\mathrm{IBODCM}}}=\frac{D_1}{D_1-D}\eta_{\mathrm{BODCM}}$$

$$=\frac{D_1}{D_1-D}\left\{1+\frac{V_{\mathrm{F}}}{V_{\mathrm{O}}}+[R_{\mathrm{L}}D_1+R_{\mathrm{DS}}D+R_{\mathrm{F}}(D_1-D)+R_{\mathrm{C}}(D_1-D)]\frac{V_{\mathrm{I}}^2}{V_{\mathrm{O}}I_{\mathrm{O}}}\frac{D^2}{3L^2f^2}\right.$$

$$\left.+R_{\mathrm{C}}\left[\frac{I_{\mathrm{O}}}{V_{\mathrm{O}}}-\frac{V_{\mathrm{I}}D(D_1-D)}{V_{\mathrm{O}}Lf}\right]+\frac{5}{24}\frac{V_{\mathrm{I}}D}{LfI_{\mathrm{O}}}(t_{\mathrm{r}}+t_{\mathrm{f}})f\right\}^{-1} \tag{49}$$

Figure 16 shows the efficiency of a DC–DC buck converter operated in the DCM at a constant output voltage $V_{\mathrm{O}}=48\,\mathrm{V}$ and at a full load current $I_{\mathrm{O}}=0{\cdot}65\,\mathrm{A}$, evaluated by substituting (46) in (48). The switching frequency was $f=10\,\mathrm{kHz}$, the rise and fall times $t_{\mathrm{f}}=t_{\mathrm{r}}=150\,\mathrm{ns}$, the inductor had an inductance $L=10\,\mu\mathrm{H}$ and an ESR $R_{\mathrm{L}}=300\,\mathrm{m\Omega}$, the MOSFET drain-to-source resistance was $R_{\mathrm{DS}}=55\,\mathrm{m\Omega}$, the capacitor ESR $R_{\mathrm{C}}=50\,\mathrm{m\Omega}$, the voltage of the battery used in the diode model was $V_{\mathrm{F}}=0{\cdot}57\,\mathrm{V}$ and the resistance $R_{\mathrm{F}}=25\,\mathrm{m\Omega}$. In Fig. 17 the ideal voltage transfer function is compared to that given by (49).

3. Validation of the theoretical derivations

Computer simulations of the buck and boost converters operated both in the CCM and in the DCM were used to validate the theoretical derivations. The circuit

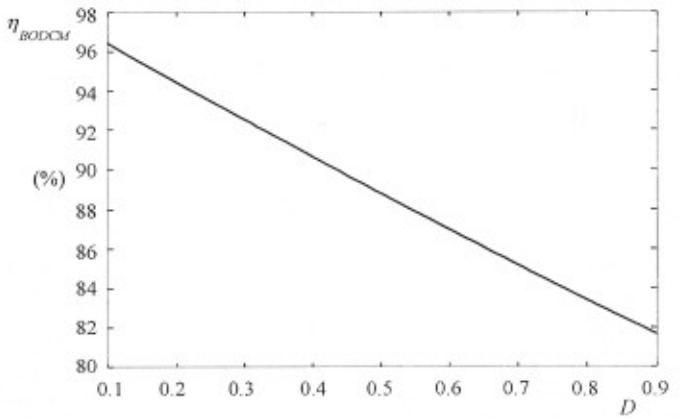

Figure 16. Efficiency η_{BODCM} of a boost converter operated in the DCM, a constant output voltage $V_{\mathrm{O}}=48\,\mathrm{V}$ as a function of the duty cycle D at $I_{\mathrm{O}}=0{\cdot}65\,\mathrm{A}$, $f=10\,\mathrm{kHz}$, $R_{\mathrm{DS}}=55\,\mathrm{m\Omega}$, $t_{\mathrm{r}}=t_{\mathrm{f}}=150\,\mathrm{ns}$, $V_{\mathrm{F}}=0{\cdot}57\,\mathrm{V}$, $R_{\mathrm{F}}=25\,\mathrm{m\Omega}$, $L=10\,\mu\mathrm{H}$, $R_{\mathrm{L}}=300\,\mathrm{m\Omega}$ and $R_{\mathrm{C}}=50\,\mathrm{m\Omega}$.

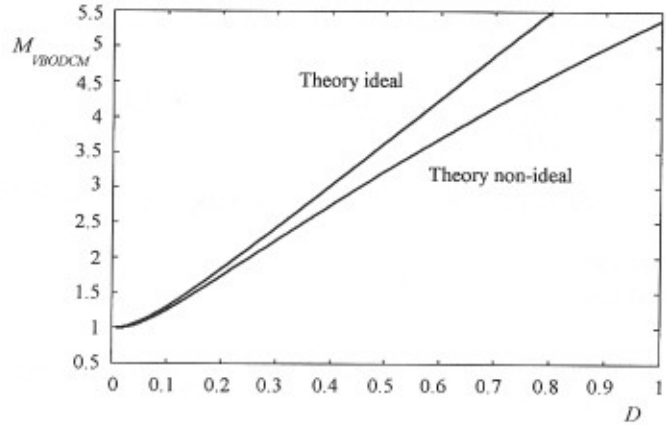

Figure 17. Voltage transfer function M_{VBODCM} of a boost converter operated in the DCM, a constant output voltage $V_O = 48\,V$ as a function of the duty cycle D at $I_O = 0{\cdot}65\,A$, $f = 10\,kHz$, $R_{DS} = 55\,m\Omega$, $t_r = t_f = 150\,ns$, $V_F = 0{\cdot}57\,V$, $R_F = 25\,m\Omega$, $L = 10\,\mu H$, $R_L = 300\,m\Omega$ and $R_C = 50\,m\Omega$.

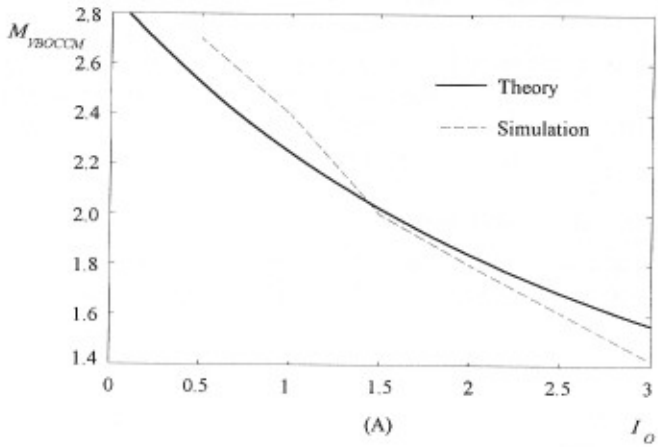

Figure 18. Voltage transfer function M_{VBOCCM} of a boost converter operated in the CCM, a constant output voltage $V_O = 12\,V$ as a function of the DC output current I_O at a duty cycle $D = 0{\cdot}7$ and a switching frequency $f = 100\,kHz$.

of Fig. 12(*b*) was simulated by using the PSpice program. The values of the series resistances of inductor L and capacitor C were chosen according to those given in section 2.4. The model of the IRF150 power MOSFET given in the PSpice library was used to simulate the controlled switch. Data sheets give $R_{DS} = 55\,m\Omega$ and $t_r = t_p = 100\,ns$ for the IRF150 power MOSFET. The default PSpice diode model was utilized: it had $V_F = 1{\cdot}66\,V$ and $R_F = 30\,m\Omega$. During the simulations the input voltage was changed so that the output voltage was kept constant and equal to 12 V for different values of the load resistance, that is, a constant output voltage operation was simulated with different values of the input voltage V_I and output current I_O.

Figure 18 compares the voltage transfer function of the boost converter operated in the CCM evaluated using (49) and that resulting from computer simulations. In

Fig. 19 the efficiency given by (48) is compared with that obtained by simulating the converter circuit of Fig. 10(*b*).

4. Conclusions

Expressions for the efficiencies and voltage transfer functions of the two basic PWM DC–DC buck and boost converters have been derived by means of a detailed time-domain analysis. Switching losses in the power MOSFET used as a controlled switch have been considered along with conduction losses in the inductors, capacitors, diodes and MOSFETS. The effect of the inductor current ripple has been taken into account so that the expressions for the efficiencies and voltage transfer functions have been derived in a closed form for both CCM and DCM operations. The derivations presented yield equations for the voltage transfer functions of the buck and boost PWM converters which depend on the load variations in CCM operation in the same way as in the actual converter circuits. It has been shown that for a buck converter operated in the CCM at a constant input voltage low values of the duty cycle result in a poor load regulation capability. Similarly, for a boost converter operated in the CCM at a constant output voltage, the voltage transfer function increases only when the duty cycle varies from zero to a certain value (lower than one, determined by the operating conditions), and then decreases to zero for values of the duty cycle approaching one. All of this is closely reflected by the results of the analysis presented.

In addition, equations for the efficiencies and voltage transfer functions of buck and boost converters have been derived so that the values of parasitic parameters can be easily read from component data sheets or derived by simple measurements. Moreover, general expressions for these equations are presented so that they can be applied to buck and boost converters operated under any conditions, That is, they are suitable for describing the converter circuit behaviour in DCM and CCM operation and at a constant output, and input voltage.

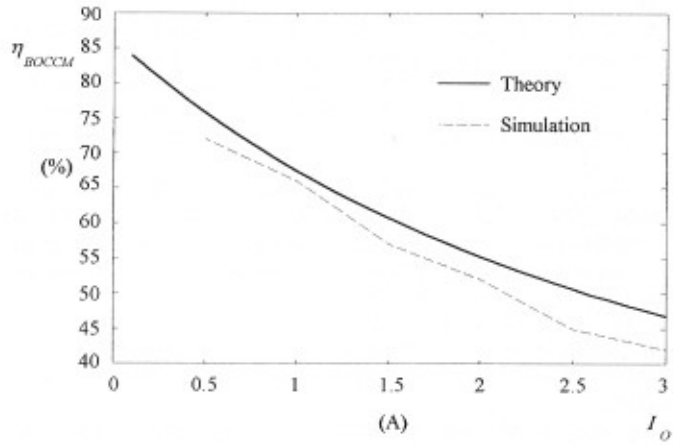

Figure 19. Efficiency η_{BOCCM} of a boost converter operated in the CCM, a constant output voltage $V_O = 12$ V as a function of the DC output current I_O at a duty cycle $D = 0{\cdot}7$ and a switching frequency $f = 100$ kHz.

The results of the analysis presented allow parameters like the duty cycle, the switching frequency etc., and the component values to be chosen accurately so that the converter can be operated with the highest efficiency for any given application. Therefore, they represent a helpful tool for power converter design optimizations. In future work, the analysis presented will be extended to the buck and boost derived topologies.

References

Amran, Y., Huliehel, H., and Ben-Yaakov, S., 1991, A unified SPICE compatible averaged model of PWM converters. *IEEE Transactions on Power Electronics*, **6,** 585–594.

Billings, K. H., 1989, *Handbook of Switchmode Power Supplies*, edited by D. A. Gonneau and S. Thomas (New York: McGraw-Hill).

Bracke, L. P. M., and Geerling, F. C., 1986, High frequency ferrite power transformer and choke design, parts 1 and 2. *Philips Technical Papers TP205 and TP206*.

Czarkowski, D., and Kazimierczuk, M. K., 1992 a, Linear circuit models of P.W.M. flyback and buck/boost converters. *IEEE Transaction on Circuits and Systems—Part 1: Fundamental Theory and Applications*, **39,** 688–693; 1992 b, Linear circuit models of P.W.M. dc–dc converters. *Proceedings of the IEEE National Aerospace and Electronics System Conference (NAECON)*, Dayton, Ohio, U.S.A., 18–22 May 1992, pp. 407–413; 1992 c, SPICE compatible averaged models of P.W.M. full bridge dc–dc converters. *Proceedings of the Electronics, Control and Instrumentation Conference (IECON)*, Dayton, Ohio, U.S.A., 18–22 May 1992, pp. 488–493; 1992 d, Circuit models of PWM half-bridge dc–dc converter. *Proceedings of 35th Midwest Symposium on Circuits and Systems*, Washington, DC, U.S.A., 9–12 June 1992, pp. 469–472; 1992 e, A new and systematic method of modelling P.W.M. DC–DC converters. *Proceedings of the IEEE Conference on Systems Engineering*, Kobe, Japan, 17–19 September 1992; 1992 f, Static- and dynamic-circuit models of P.W.M. buck derived DC–DC converters. *Proceedings of the Institution of Electrical Engineers*, Pt G, **139,** 669–679; 1993, Energy-conservation approach to modelling P.W.M. DC–DC converters. *IEEE Transactions on Aerospace and Electronic Systems*, **29,** 40–41.

Fisher, M. J., 1991, *Power Electronics*, edited by J. Plant (Boston, Mass: PWS-Kent).

Kassakian, J. C., Schlecht, M. F., and Verghese, G. C., 1991, *Principles of Power Electronics*, first edition (New York: Addison-Wesley).

Kazimierczuk, M. K., Szaraniec, W., and Wang, S., 1992, Analysis and design of parallel resonant converter at high Q_L. *IEEE Transactions on Aerospace and Electronic Systems*, **28,** 35–50.

Kazimierczuk, M. K., Thirunarayan, N., and Wang, S., 1993, Analysis of series parallel resonant converter. *IEEE Transactions on Aerospace and Electronic Systems*, **29,** 88–99.

Kazimierczuk, M. K., and Wang, S., 1992, Frequency domain analysis of series converter for continuous conduction mode. *IEEE Transactions on Power Electronics*, **7,** 270–279.

Kilgenstein, O., 1989, *Switched-Mode Power Supplies in Practice*, first edition (New York: Wiley).

Lee, Y. S., 1985, A systematic and unified approach to modelling switches in switch-mode power supplies. *IEEE Transactions on Industrial Electronics*, **32,** 445–448.

Liberatore, A., and Reatti, A., 1993, Efficiency optimization of the transformer of a flyback converter. *Proceedings of the Third European Space Power Conference (ESPC93)*, Graz, Austria, 23–27 August 1993, pp. 173–179.

Middelbrook, R. D., and Ćuk, S., 1981, *Advances in Switched Mode Power Conversion*, Vols I and II (Pasadena, California: TESLAco).

Mitchell, D. M., 1988, *Switching Regulators Analysis*, first edition (New York: McGraw-Hill).

Mohan, M., Undeland, T. M., and Robbins, W. P., 1989, *Power Electronics: Converters, Application and Design*, first edition (New York: Wiley).

Pressmann, A. I., 1991, *Switching Power Supply Design*, second edition, edited by D. A. Gonneau (New York: McGraw-Hill).

REATTI, A., and KAZIMIERCZUK, M. K., 1993 a, Efficiency of the transformer version of the class E half-wave low dv_D/dt *rectifier. Proceedings of the IEEE International Symposium on Circuits and Systems (ISCAS)*, Chicago, Illinois, U.S.A., 3–6 May 1993, pp. 2331–2334; 1993 b, Comparison of the efficiencies of Class D and Class E rectifier. *Proceedings of the 36th Midwest Symposium on Circuits and Systems*, Detroit, Michigan, U.S.A., 16–18 August 1993, Vol. 2, pp. 871–874.